Model-Based Damage Identification in a Continuous Bridge Using Vibration Data

Ashutosh Bagchi[1]; Jag Humar[2]; Hongpo Xu[3]; and Ahmed S. Noman[4]

Abstract: Damage often causes changes in the dynamic characteristics of a structure such as frequencies and mode shapes. Vibration-based damage identification techniques utilize the changes in the dynamic characteristics of a structure to determine the location and extent of damage in the structure. Such techniques are applied in this study to the Crowchild Bridge, a steel-free deck continuous bridge located in western Canada. While the numerical models of the bridge are correlated with the measured dynamic characteristics, computer simulation is used to study the identification of a number of different damage patterns, and the effects of measurement errors and incomplete mode shapes on the quality of results are evaluated. The effectiveness of some selected damage identification techniques is examined; the potential difficulties in identifying the damage are outlined; and areas of further research are suggested. A three-dimensional finite-element model and a simple two-dimensional girder model of the bridge have been constructed to study the usefulness of the selected damage identification methods. Another promising damage detection method proposed here is based on the application of neural networks that combines a vibration-based method.

DOI: 10.1061/(ASCE)CF.1943-5509.0000071

CE Database subject headings: Vibration; Damage; Structural reliability; Monitoring; Neural networks; Continuous structures; Bridges; Canada.

Author keywords: Vibration-based damage identification; Structural health monitoring; Steel-free deck; Artificial neural network.

Introduction

Structural health monitoring (SHM) is a powerful tool for the maintenance and management of large civil engineering structures. Vibration-based damage identification (VBDI) techniques are cost effective and easy to implement means of structural condition assessment of civil engineering structures. As the vibration characteristics such as frequencies and mode shapes are global properties that change when the structure suffers damage, it should be possible to determine the location and severity of the damage based on their differences between a healthy and a damaged structure. Vibration-based assessment offers several advantages, one of which is that the location of damage need not be known beforehand. The sensors required to measure the vibration characteristics need not be located in the vicinity of the damage, and a limited number of sensors can, at times, provide sufficient information to locate the damage and assess its severity. Vibration measurements can be a part of continuous remote monitoring facilitating the development of an early warning system and efficient management of maintenance schedules. However, in practice, the VBDI techniques have a number of problems including effect of measurement errors, availability of only incomplete mode shapes, mode truncation, nonunique nature of the solutions, and environmental factors. These difficulties are particularly severe for civil engineering structures.

This paper presents the application of vibration-based structural damage identification techniques in health monitoring of the Crowchild Bridge, a three-span continuous bridge with an innovative steel-free deck (Bakht and Mufti 1998), constructed under the technical advice of ISIS Canada, a Canadian Network of Center of Excellence. The bridge is located in Calgary, Alberta. Innovative techniques and materials have been used in the construction of this bridge. Sensors for measuring strain and temperature have been installed in the structure to facilitate remote monitoring of the structural health. The expectation is that the data collected from the sensors will be helpful in evaluating the extent and location of any damage in the structure. A preliminary study on the damage identification of the Crowchild Bridge can be found in Humar et al. (2003).

Computer simulation is used to study the identification of a number of potential damage patterns in the bridge and to evaluate the effects of measurement errors and incomplete mode shapes on the quality of results. A finite-element (FE) model of the bridge is developed and updated and correlated with available vibration test data on the structure at the initial phase (i.e., 1997) when the bridge is opened. At this time the structure is assumed to be undamaged (although it is difficult to verify). This model will be referred to as the "baseline structure." The damage in an element is simulated by reducing its stiffness by a specified ratio. A revised FE model is then constructed and used to obtain the ana-

[1]Associate Professor, Dept. of Building, Civil and Environmental Engineering, Concordia Univ., 1455 de Maisonneuve Blvd. West, EV-6.111, Montreal PQ, Canada (corresponding author). E-mail: abagchi@bcee.concordia.ca

[2]Distinguished Research Professor, Dept. of Civil and Environmental Engineering, Carleton Univ., Ottawa ON, Canada K1S 5B6.

[3]Facilities Engineer, Fisheries and Oceans Canada, St. Andrews NB, Canada E5B 2L9.

[4]Project Manager, Basic Consultant Limited, Dhaka, Bangladesh; formerly, Graduate Student, Dept. of Building, Civil and Environmental Engineering, Concordia Univ., Montreal PQ, Canada H3G 1M8.

Note. This manuscript was submitted on November 11, 2008; approved on July 1, 2009; published online on March 15, 2010. Discussion period open until September 1, 2010; separate discussions must be submitted for individual papers. This paper is part of the ***Journal of Performance of Constructed Facilities***, Vol. 24, No. 2, April 1, 2010. ©ASCE, ISSN 0887-3828/2010/2-148–158/$25.00.

lytical mode shapes and frequencies of the damaged structure. These analytical mode shapes are then reduced in size based on a selected practical placement of sensors to simulate the availability of only incomplete mode shapes. The incomplete mode shapes are expanded to the full size using a modal expansion technique. Random errors are introduced in the incomplete modes to simulate the noise in measured quantities. The effectiveness of selected VBDI techniques is studied; at the same time the potential difficulties are identified and possible areas of further research are suggested.

The results of the simulation suggest that the damage detection algorithms are sensitive to the spatial incompleteness of the mode shape vectors and the measurement errors. Two different damage identification techniques are applied to the Crowchild Bridge and when the results of both the methods are synthesized together, it is possible to get an idea about the damage location and severity in spite of the difficulties associated with these techniques.

Artificial neural networks originally developed to simulate the function of the human brain are computational models. In recent years there has been an increasing interest in using artificial neural networks to detect damage in complex structures (e.g., Zang and Imregun 2001; Humar et al. 2004; Xu and Humar 2006). In the present work the modal strain energy concept of structural dynamics is combined with artificial neural network technique to detect damage. The structural damage detection problem is, in fact, divided into two distinct subproblems. In the first step, the damage location is obtained by using the strain energy method. In the second step, the damage magnitude is evaluated by applying an artificial neural network technique. It is shown that the proposed method is practical and effective.

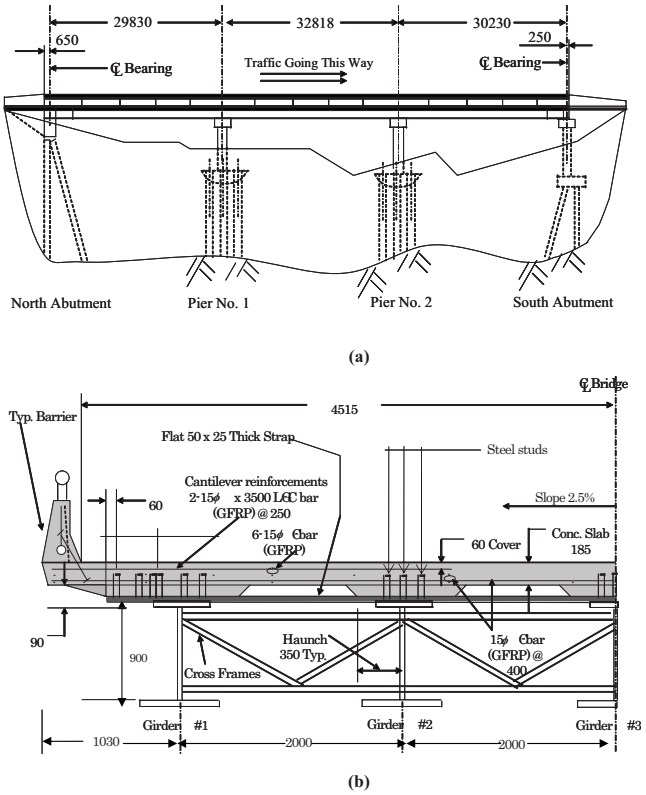

Fig. 1. Details of the Crowchild Bridge—(a) west elevation; (b) cross section

Details of the Crowchild Bridge

The Crowchild Bridge located in Calgary, Alberta is a two-lane traffic overpass with three continuous spans. The details of the bridge superstructure are shown in Fig. 1. The superstructure is said to be the first continuous-span steel-free bridge deck in the world (Tadros et al. 1998). It comprises five longitudinal steel girders (900 mm or 35.4 in. deep), a polypropylene fiber reinforced concrete slab deck and prefabricated glass fiber reinforced concrete barriers. The five longitudinal girders are spaced at 2 m (6.6 ft) apart. Four evenly spaced cross-frames in each span and steel girder diaphragms at the supports hold the main girders in place. The main girders are also connected by evenly spaced steel straps placed across the top of the girders to provide lateral restraint to them. The girders and straps are connected to the deck slab by stainless steel stubs. The deck is 9 m (29.6 ft) wide and does not contain any internal steel reinforcement. The slab haunch thickness is 275 mm (10.8 in.) along the girders and 185 mm (7.3 in.) elsewhere.

A monitoring program for the bridge has been developed by ISIS Canada. Static and ambient vibrations tests have been conducted on the bridge by the University of British Columbia in 1997 (Ventura et al. 2000) and the University of Alberta in 1998 (Cheng and Afhami 1999) and 2004 (Cheng and Zwol 2005).

VBDI Techniques

A number of techniques for VBDI are available in the literature (Kabe 1985; Farrar et al. 1994; Doebling et al. 1998; Humar et al. 2006). They include the following: (1) methods based on frequency sensitivity; (2) methods based on modal sensitivity; (3) mode shape curvature method; (4) methods based on change in flexibility matrix; (5) methods based on changes in uniform flexibility shape curvature; (6) strain energy-based damage index method; (7) method based on modal residual vector; (8) matrix update methods; and (9) neural network methods. Here, the strain energy-based damage index method and matrix update methods are used because of their relative advantages (Humar et al. 2006).

Method Based on Modal Strain Energy

This method as originally developed by Stubbs et al. (1995) is applicable to beam-type structures and is based on the comparison of modal strain energy before and after damage. The method can be extended to a structure of a general type, details of which can be found in Humar et al. (2006). The key elements of the method are described here.

The damage index γ_j of an element in a structure is defined as the ratio of the fractional strain energy of the element in the damage state to that at the healthy state as given in Eq. (1), where the suffices i and j indicate the mode and element number, respectively; superscript d indicates the damaged state; and nm indicates the total number of measured modes

$$\gamma_j = \sum_{i=1}^{nm} f_{ij}^d / \sum_{i=1}^{nm} f_{ij} \tag{1}$$

The modal strain energy fractions (i.e., ratio of the element level strain energy and the total strain energy of the structure) of member j in mode i for the undamaged (or baseline) and damaged structure, f_{ij} and f_{ij}^d, respectively.

Numerical problems may arise in the evaluation of Eq. (1) when the denominator is very small in magnitude, which may be the case when the strain energy contributed by the jth member in the modes being considered is very small. In such a case a modified damage index $\bar{\gamma}_j$ can be defined as follows:

$$\bar{\gamma}_j = \left(1 + \sum_{i=1}^{nm} f_{ij}^d\right)\left(1 + \sum_{i=1}^{nm} f_{ij}\right) \tag{2}$$

In this case, the modified damage index $\bar{\gamma}_j$ gives a value close to 1 when there is no or negligible amount of damage.

For a beam-type structure, the modal curvatures can be used to calculate the modal strain energies. In the field, the modal curvature at a section of the girder can be measured by attaching strain gauges capable of measuring dynamic strains at two or more points over the depth of the section. With the progress in sensor technology and the development of fiber optic sensors, measurement of dynamic strains has become quite feasible. Using modal curvatures, ψ'', the damage index γ_{ij} for element j in mode i is obtained from Stubbs et al. (1995)

$$\gamma_{ij} = \frac{\int_a^b [\psi_i^{d''}(x)]^2 dx \Big/ \int_0^L EI(x)[\psi_i^{d''}(x)]^2 dx}{\int_a^b [\psi_i''(x)]^2 dx \Big/ \int_0^L EI(x)[\psi_i''(x)]^2 dx} \tag{3}$$

where x=coordinate along the length of the beam; L=total length of the beam; E=modulus of elasticity; I=moment of inertia; and a and b=distance of the two ends of an element from the origin; subscript i indicates the mode number in question and superscript d indicated the damaged structure.

Matrix Update Methods

The matrix update method as developed by Kabe (1985) has been adapted here for damage identification. While a detailed description of the method is available in Humar et al. (2006), the key relation between the perturbation in stiffness matrix and the modal parameters at the healthy and damaged states is given below

$$\sum_{j=1}^{ne} \phi_i^T \mathbf{k}_j \phi_{di} \beta_j = -\delta\lambda_i \phi_i^T \mathbf{M} \phi_{di} \tag{4}$$

where β_j=damage factor for element j, which quantifies the perturbation in the element stiffness matrix $\mathbf{k}_j$; and λ_i=ith eigenvalue. Eq. (4) can be rewritten as

$$\mathbf{D}\beta = \mathbf{C} \tag{5}$$

where ne=number of members and $\mathbf{D}$=an m by ne matrix whose elements are given by

$$d_{ij} = \phi_{di}^T \mathbf{k}_j \phi_{di} \tag{6}$$

β=ne-vector of the unknown changes in element stiffness matrices; $\delta\lambda_\iota$=change in the eigenvalue corresponding to the ith mode; and $\mathbf{C}$=vector of eigenvalue perturbation as defined by the right-hand side of Eq. (4).

Solution of Eq. (5) provides both the location and severity of the damage. A simple inversion of the $\mathbf{D}$ matrix is not possible as it is not a square matrix. A pseudo-inverse solution of Eq. (5) is possible by premultiplying both sides by $\mathbf{D}^T$ to convert the coefficient matrix on the left-hand side to a square one. On the other hand, a unique solution can be obtained through the minimization of an objective function subject to some specified constraints.

There are many different ways in which the objective function and constraints can be defined and the different numerical techniques that can be used in the solution of the resulting optimization problem. A method using the minimization of the quadratic norm of the stiffness changes given by Eq. (7) is chosen in the present work

$$J = \beta^\tau \beta \tag{7}$$

The solution of Eq. (5) is obtained here by minimizing J in Eq. (7) subjected to a constraint as defined in Eq. (8)

$$0 \le \beta_j \le 1 \tag{8}$$

The optimization technique used in the present work is based on a sequential quadratic programming (SQP) method using MATLAB (2009). Gill et al. (1981) provided an overview of the SQP method.

When a system involves a large number of elements, the optimization process would require a long time to complete. In addition, many times when the incomplete mode shapes are used and random noise exists in the measured data, the optimization process fails to converge to a stable solution. The process is proposed to be accelerated by excluding from consideration those elements that are not likely to have been damaged and formulating the problem in terms of a smaller set of potentially damaged elements (reduced system). A damage localization algorithm such as the strain energy-based damage index method is used here for identifying the potentially damaged elements that should be included in the reduced system.

Artificial Neural Network Technique

Artificial neural networks have been developed to parallel the biological neural networks. The basic processing unit in the network is called a neuron, which are usually organized into groups called layers. The neurons are interconnected to form a network and each neuron performs a simple mathematical operation called activation function. The weighted sum of the output data received from all neurons in a layer forms an input vector to the subsequent layer. To this sum is added a bias, which is formed by multiplying a constant input, usually a vector of 1, and a vector of bias weights. As an illustration consider the feedforward network used in the present work and shown in Fig. 2. It consists of two layers of neurons, a hidden layer, and an output layer. The hidden layer, which is also the first layer, has 30 neurons. Neurons in the layer receive their signals from a 15-element input vector $\mathbf{P}$. These signals are multiplied by matrix $\mathbf{W}^1$ to form $\mathbf{W}^1\mathbf{P}$, which is one of the terms sent to the summers in the neurons. The other input vector, whose elements are all 1, is multiplied by a bias vector $\mathbf{b}^1$ and then passed to the summers. The sum of these two terms becomes the net input to the activation functions $\mathbf{f}^1$, which produce the output vector $\mathbf{a}^1$. The second layer, which in this case is also the output layer, contains only one neuron. It receives weighted signals $\mathbf{W}^2\mathbf{a}^1$ and $\mathbf{b}^2$, adds the two, and produces the output.

The feedforward neural network can be regarded as a nonlinear mathematical function, which transforms a set of input variables into a set of output variables. The transformation is governed by a set of parameters, namely, the weight matrices and the bias vectors. These parameters are adjusted such that when provided with a given input data the network produces an output

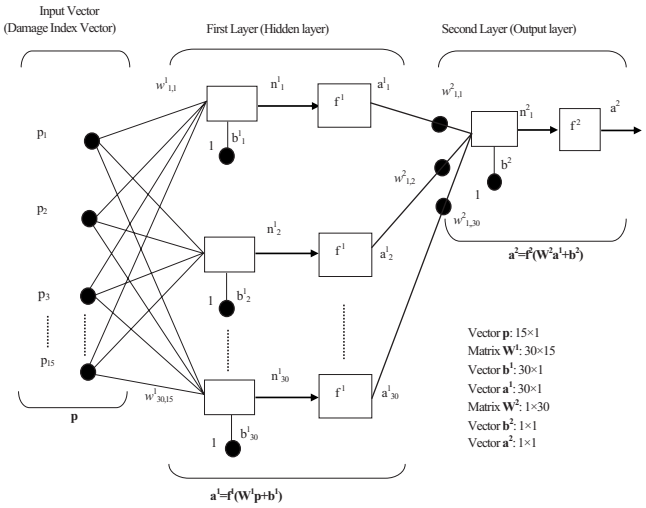

Fig. 2. Feedforward neural network

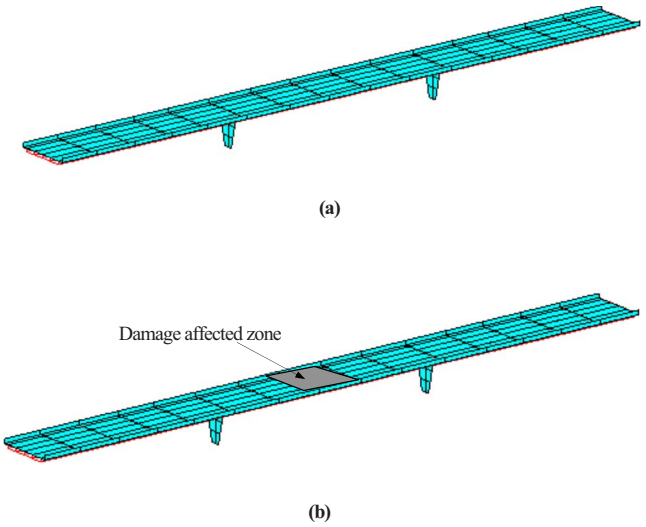

Fig. 3. (a) FE model of Crowchild Bridge; (b) damaged area for computer simulation

that closely matches the expected results. The process of determining the values of the parameters is often called learning or training. Training thus requires a set of input data for which the output is known. Once the weights and the biases have been appropriately fixed, new input data for which the outputs are known are used for validation of the trained network.

The training of neural network is a process of optimizing the weight matrices and the bias vectors to minimize some specified error function, such as the sum of the squared error between the actual output and the corresponding target output of the neural network. A large number of training algorithms have been developed for feedforward neural networks. The most fully developed and commonly used is back-propagation algorithm. Within the back-propagation training a variety of training algorithms have been employed; the one used in the present work is the scaled conjugate gradient algorithm. A detailed description of the algorithm can be found in Hagan et al. (1995). An implementation of this algorithm that exists in the computer software MATLAB (2009) is used in this work.

Training of neural networks is an iterative process in which the parameters are adjusted over a number of iterations until the output and target vectors match within a specified tolerance. If this process is continued too long, the network while being very accurate in reproducing the desired output for the data used in training, loses some of its ability to accurately process new data. To avoid such overfitting and to increase the generalization capability of the neural network, a validation data set is employed in this research. The error on the validation set is monitored during the training process. The validation error will first decrease, as does the training set error. When the network begins to overfit the training data, the error on the validation set becomes unstable. If the validation error keeps increasing for a specific number of consecutive iterations, the training is stopped, and the weights and biases when the validation error is the minimum are returned.

The training of the neural network with appropriate data is a critical part of the proposed method of damage assessment. In the present study the damage index vectors for a variety of specified locations and magnitudes of damage are used as the input for training the network to predict the extent of damage. Such data can be generated through measurement of structural response over time, model test results, or through numerical simulation, or a combination of all three. In this study, the training samples are generated from the damage factors obtained through computer simulation. Such damage factors are calculated for a range of element damage magnitudes between 0 and 60% represented by a corresponding decrease in the stiffness of the elements.

FE Model

The bridge structure is modeled using a MATLAB based FE program, M-FEM, developed by Bagchi et al. (2007) which implements the damage detection methods discussed earlier. The element library in M-FEM includes the plate-shell and three-dimensional (3D) beam elements. The plate and shell element is formed using the triangular plate bending element called the discrete Kirchoff triangle element (Batoz 1982) and the plane stress element with drilling degrees of freedom (Allman 1984).

A FE model of the Crowchild Bridge is constructed using 3D beam elements for the piers, girders, diaphragms, and the cross-frames including the steel straps, and shell elements for the deck and side barriers. The deck elements are connected to the girder elements by rigid beam elements. The piers are assumed to be fixed at their base, while roller and pin supports are assumed to exist at the north and south abutments, respectively. The FE model contains 351 elements, 247 nodes, and 1399 active degrees of freedom. The density of steel and concrete is assumed to be 76 and 24 kN/m^3, respectively. The concrete compressive strength is taken as 35 MPa. The modulus of elasticity for concrete is assumed to be 30 GPa for the deck and 27 GPa for the barrier and pier; for steel it is assumed to be 200 GPa. The FE model of Crowchild Bridge is shown in Fig. 3(a), and the damage area assumed for computer simulation is shown in Fig. 3(b). Many static, dynamic, and ambient vibration tests have been carried out on the structure in 1997 (Ventura et al. 2000), 1998 (Cheng and Afhami 1999), and 2004 (Cheng and Zwol 2005). The natural frequencies of the structure obtained from these tests are reported in Table 1.

The model of the as-built structure is updated and correlated with the data obtained from the vibration test conducted in 1997 by the University of British Columbia (Ventura et al. 2000) and is used as the baseline model of the structure. The model updating and correlation are carried out by using the procedure described

Table 1. Natural Frequencies of the Crowchild Bridge

Mode	Measured frequencies			Description
	1997	1998	2004	
1	2.78	2.60	2.80	First vertical mode
2	3.13	2.90	3.16	First torsional mode
3	3.76	3.63	3.78	Second vertical mode
4	4.05	3.85	4.19	Second torsional mode
5	4.64	2.43	4.66	Third vertical mode
6	5.18	5.00	5.36	Third torsional mode
7	7.13	6.85	6.89	Fourth torsional mode
8	9.13	8.60	8.29	Fourth vertical mode

in Bagchi (2005). During the process of model update, the stiffness coefficients of individual elements are modified to fine tune the resulting modal frequencies of the structural system. The mode shapes derived from the baseline model are shown in Fig. 4.

A field test conducted by the University of Alberta team in 1998 (Cheng and Afhami 1999) revealed that the frequencies of the bridge reduced slightly due to some cracking of concrete. Since both the field tests (1997 and 1998) were carried out in the summer periods (August) under similar climatic conditions, the observed reduction in frequencies is most likely due to the cracking of concrete. However, the environmental effects such as temperature changes could play a role in the reduction of the frequencies as well. The tests conducted in 2004 indicated the natural frequencies of the structure increased slightly perhaps due to temperature effect and support conditions (Cheng and Zwol 2005).

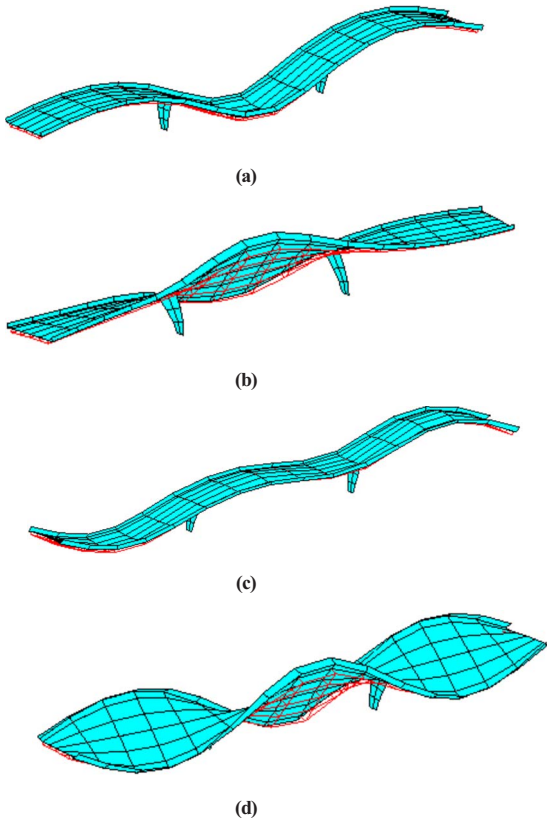

Fig. 4. Mode shapes—(a) Mode 1; (b) Mode 2; (c) Mode 3; and (d) Mode 4

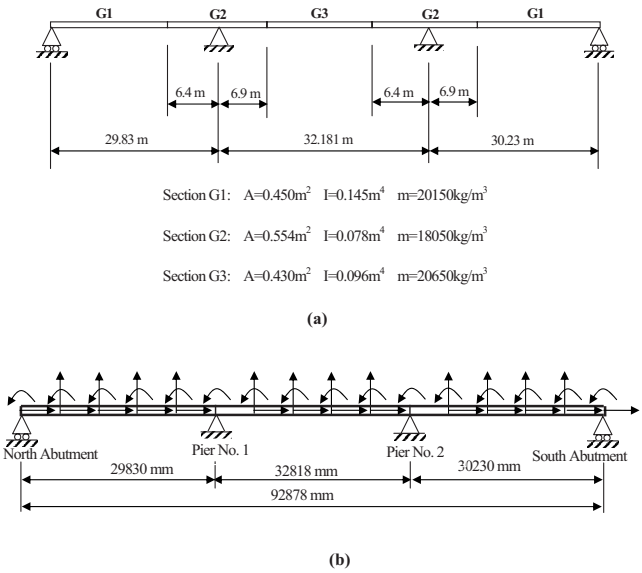

Fig. 5. Girder model of the Crowchild Bridge; (a) section properties; (b) elements and degrees of freedom

Simplified Model

A simplified model of the bridge is constructed as a continuous steel girder comprising three types of sections, G1, G2, and G3, as shown in Fig. 5. The properties of the equivalent steel girder sections are first calculated from the details of the uncracked bridge deck and the barriers and subsequently adjusted manually so that the dynamic characteristics of the first three lower flexural modes match, as closely as possible, the ambient vibration measurements of the bridge (Ventura et al. 2000). In these adjustments the moment of inertia of the sections is varied to account for the fact that in the positive moment regions a part of the concrete slab contributes to the effective moment of inertia of the girder, while in the negative moment regions only the steel section is effective.

The girder model is supported on two pin supports to represent the two piers, while the supports at the north and south abutments are modeled as roller supports. The model is divided into 15 two-dimensional beam elements connected to 16 nodes. Each intermediate node has three degrees of freedom, a horizontal translation, a vertical translation, and a rotation. A pier node has only the rotational degree of freedom. Each abutment node has two degrees of freedom, a horizontal translation, and a rotation.

Damage Identification Based on the FE Model

Computer Simulation of Damage

The effectiveness of the VBDI techniques considered here has been studied by applying the techniques to detect simulated damage in the bridge models. The damage is assumed to be concentrated in the area identified in Fig. 3(b). The following scenarios are considered:

1. Damage Case D1—the longitudinal girders in the affected area (Elements 174, 177, 180, 183, and 186 in the FE model) and the deck slab over them (Element 53 through 58) are damaged by 10%; and

2. Damage Case D2—only the longitudinal girders in the affected area are damaged by 70%.

In the above damage cases, the percentage of damage is related to the loss of cross-sectional properties (thickness, area, and moment of inertia) caused by cracks and damage. For example, 10% damage in a girder element (or segment) can be interpreted as a moderate loss of the effective cross-sectional area of the girder at the corresponding location such that the flexural stiffness of the girder segment is reduced by 10% from its baseline value. Considering the flexural stiffness of a girder, which is primarily governed by the area, 10% damage would roughly indicate 10% loss of flange area for the part of the girder represented in a finite element.

The experimental frequencies and mode shapes are often corrupted by random noise. Another factor to be considered is that the FE model usually contains a large number of degrees of freedom, but in the field only a limited number of sensors could be deployed. In addition, measurement of rotational degrees of freedom is not practical. Thus only a few translation degrees of freedom are measured, and the experimental mode shapes are far from complete. This implies that either the incomplete mode shapes need to be expanded to the full size of the FE model or the FE model condensed to the measured degrees of freedom. A number of techniques are available for achieving these. In the present study, the damage structure corresponding to each damage case is simulated by modifying the baseline structure such that the stiffness of the damaged elements is reduced by the specified factors corresponding to a damage scenario. Then, the modal parameters (i.e., mode shape vectors and frequencies) of the damaged structure are generated using modal analysis. Incomplete mode shapes are constructed by selecting those elements of the analytical damaged mode shapes that correspond to a set of degrees of freedom along which measurements would be probably be made during a field test. The incomplete mode shapes are modified by adding a small amount of random perturbation to simulate the noise in measurement, which are then expanded using a method proposed by O'Callahan et al. (1989) to obtain a complete set of mode shapes for the damaged structure. Here, the incomplete mode shapes are generated from the FE model of the damaged structures by assuming that only the translation degrees of freedom at each node have been measured. The random measurement noise is assumed to be up to 2%, which is chosen arbitrarily. It means that the measured value of a certain quantity (e.g., frequency or mode shape amplitude) is up to 2% higher or lower than the actual value. It should be noted that although it is impossible to eliminate measurement noise, a high degree of accuracy of the modal data is required for the vibration-based damage detection algorithms to work as they are very sensitive to the quality of such data. Repeated measurement and averaging can reduce the effects of random errors and enhance the reliability of the measured quantities. The simulated modal parameters for the baseline and damaged structures are used for identifying the damage location and severity by using the methods discussed earlier.

Identification of Damage

In this section, selected results are presented to show the applicability of the VBDI techniques to a complex structure like the Crowchild Bridge. The modified damage index [Eq. (3)] is used for damage localization, and the matrix update method, represented by Eq. (6), is used for estimating the severity of damage. Figs. 6 and 7 show the damage identification results from the 3D FE model with Damage Case D1.

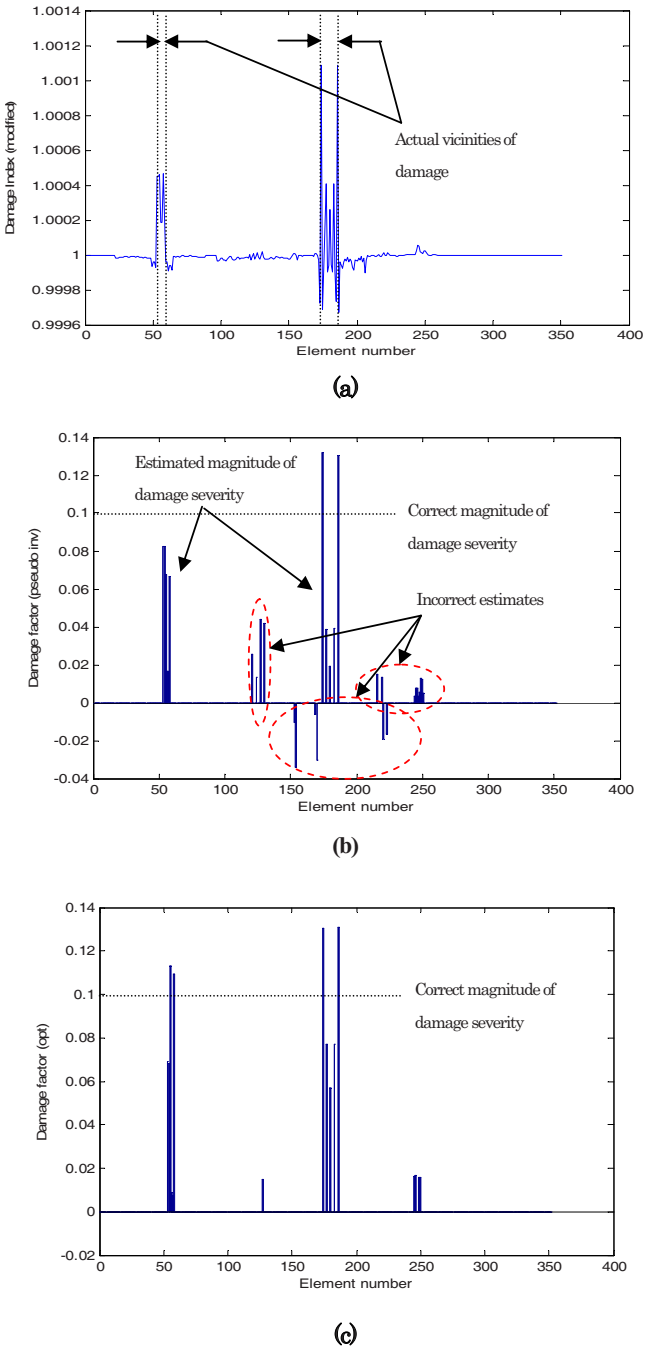

Fig. 6. Results with complete and error-free modes: (a) damage index (modified); (b) damage factors by matrix update method (pseudo-inverse); and (c) damage factors by matrix update method (optimization)—Damage Case D1

In Fig. 6, the damage indices and severity of damage presented when complete and error-free modal parameters for the damaged structure are available. Fig. 6(a) indicates the damage location in the structure determined using the modified damage indices for all the elements according to Eq. (2). On the other hand, Figs. 6(b and c) indicate the damage severity as determined using the pseudo-inverse and optimized solutions of Eq. (5), respectively. In Fig. 6(a), a positive sharp spike corresponding to an element indicates that the element is damaged. However, the severity of the damage is not clearly known from this plot. It is clear from this figure that the damage index values corresponding to the

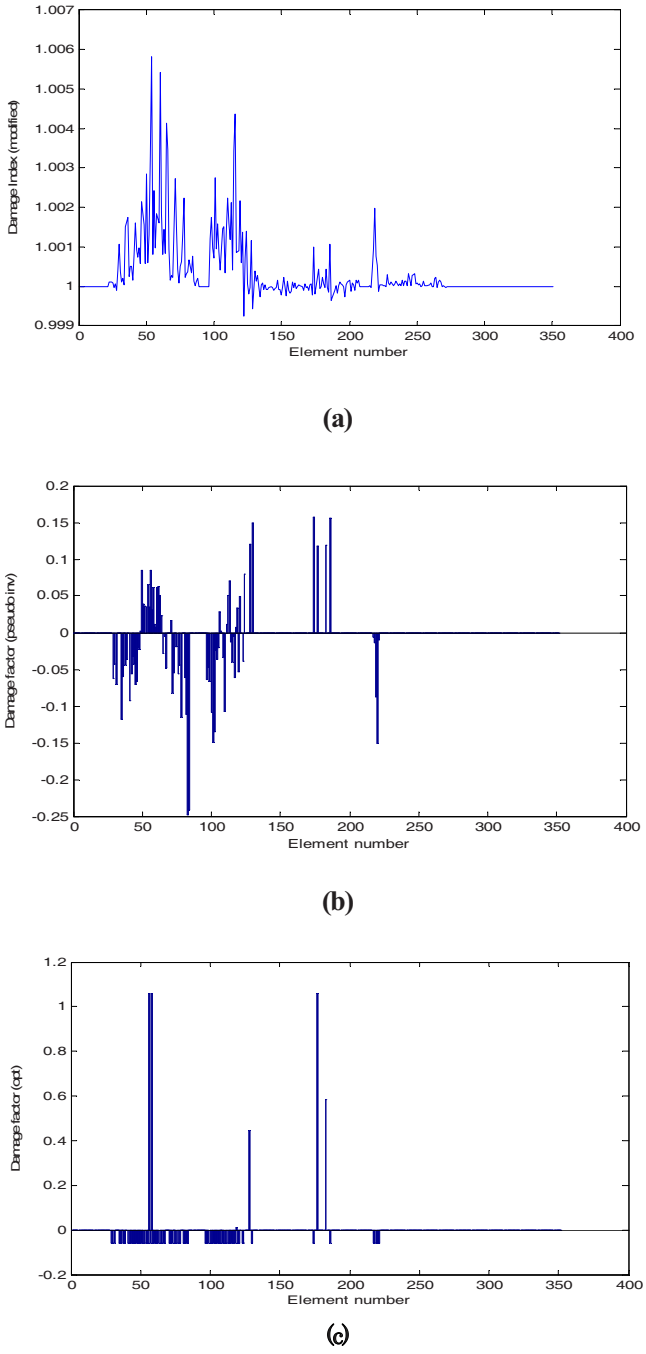

Fig. 7. Results with incomplete modes and measurement errors: (a) damage index (modified); (b) damage factors by matrix update method (pseudo-inverse); and (c) damage factors by matrix update method (optimization)—Damage Case D1

elements in the simulated damaged area (Elements 53–58 for slab and Elements 174, 177, 180, 183, and 186 for girders) are indeed high as compared to other elements, which means that these elements are identified correctly by the damage index method. In the simulation, the actual damage severity in the slab and girder elements in the affected zone as shown in Fig. 3(b) are considered to be 10%. Fig. 6(b) shows the values of the damage factor or severity, β, obtained using the pseudo-inverse solution of Eq. (5). It should be observed that in this case β can take negative values, which can be discarded as negative damage is not possible. In this figure, the value of β (i.e., height of the spike) for an element indicates the severity of damage for that element. It is observed from the figure that the estimated damage severity in the slab elements ranges from 6 to 13% (average 7.5%) and that for the girder elements ranges from 7 to 8% (average 7.5%). The damage severity estimated from the optimized solution of Eq. (5) is presented in Fig. 6(c) which indicates that damage in the slab elements ranges from 7 to 11% (average 9%) and that in the girder elements ranges from 6 to 13% (average 8%). This is an improved estimate of damage severity over that obtained by the pseudo-inverse solution of Eq. (5) [Fig. 6(b)].

As mentioned earlier, the optimization process could be very slow for a large system such as the one considered here. A reduced system constructed using only the potentially damaged elements, as determined using the damage index method, is also considered here. To identify the elements with potential damage an average value is obtained for the damage index considering all of the elements. This average provides a threshold value. Elements having a damage index that is higher than the threshold are considered to be elements with potential damage. In the present case, based on the data presented in Fig. 6(a), only 27 elements out of 351 are identified as having been potentially damaged when error free and complete mode shapes are used. Damage factors obtained by solving the optimization problem for the reduced system are almost identical to those presented in Fig. 6(c).

Fig. 7 shows the effect of incomplete mode shapes and random measurement errors or noise on damage detection. It is observed from these results that the damage detection process is severely affected by the incompleteness of mode shapes and measurement errors. However, considering the results of both the damage index method and the matrix update method together, it is still possible to determine the vicinity of damage and its severity approximately.

Figs. 8 and 9 show the results of the damage detection process for Damage Case D2. It is clear from Fig. 8 that the damage location and severity are clearly determined using the damage index [Fig. 8(a)] and matrix update method [Figs. 8(b and c)], respectively, when complete and error-free mode shape vectors are used. Although the pseudo-inverse solution in Fig. 8(b) of Eq. (5) provides an estimate of the damage extent, the optimized solution of the equation as shown in Fig. 8(c) produces a more accurate estimate of damage as in Damage Case 1 (Fig. 6). Fig. 9 shows the effect of incomplete mode shapes in the damage detection process. While the damage detection process is affected by incomplete modes and measurement errors, it is observed from Fig. 9 that their effects are not as pronounced as in Case D1 when the magnitude of damage is comparatively smaller (i.e., 10% in Damage Case D1 as compared to 70% in Damage Case D2).

Damage Localization in the Girder Model

Sample results of damage localization using the strain energy-based damage index method are shown in Fig. 10. For the girder model the curvature-based damage index as defined in Eq. (3) is used here. Fig. 10(a) shows the plot of damage index values for the case of 30% damage in Element 3, when three modes are available and curvatures are obtained by numerical differentiation of the mode shape vectors. When the modes are exact, the location is predicted accurately. However, with increasing measurement errors spurious damage is indicated in another element. Similar results were obtained for other damage scenarios. Damage indices are next calculated assuming that direct measurements are made of the curvatures. Fig. 10(b) is a plot of the damage

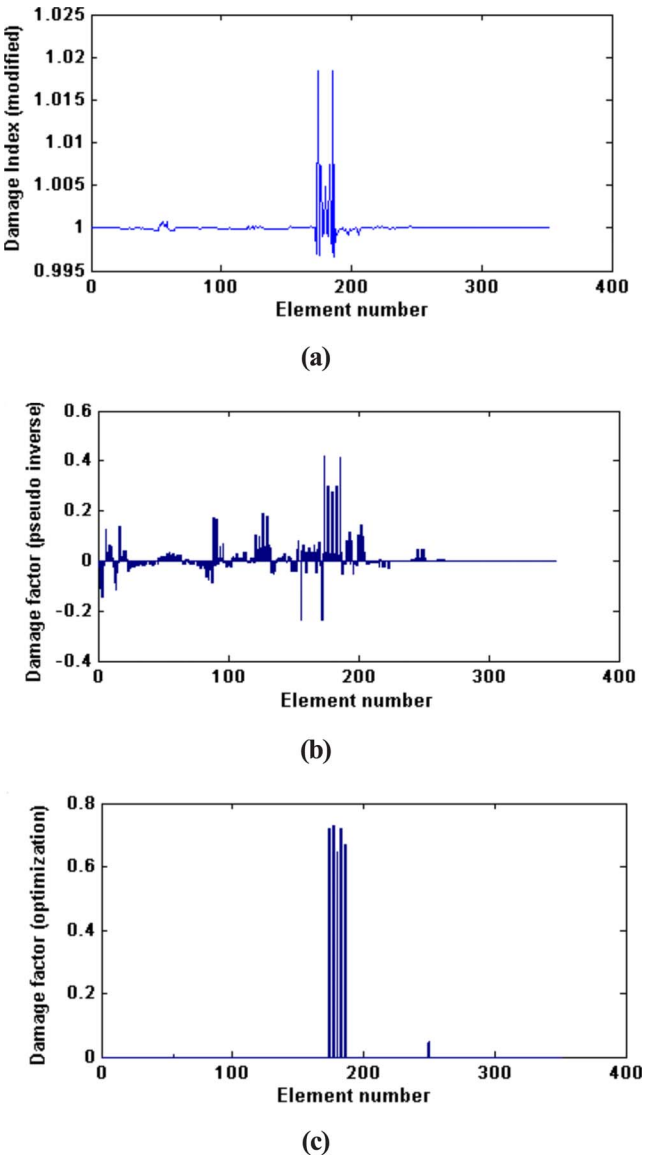

Fig. 8. Results with complete and error-free modes: (a) damage index; (b) damage factors by matrix update method (pseudo-inverse); and (c) damage factors by matrix update method (optimization)—Damage Case D2

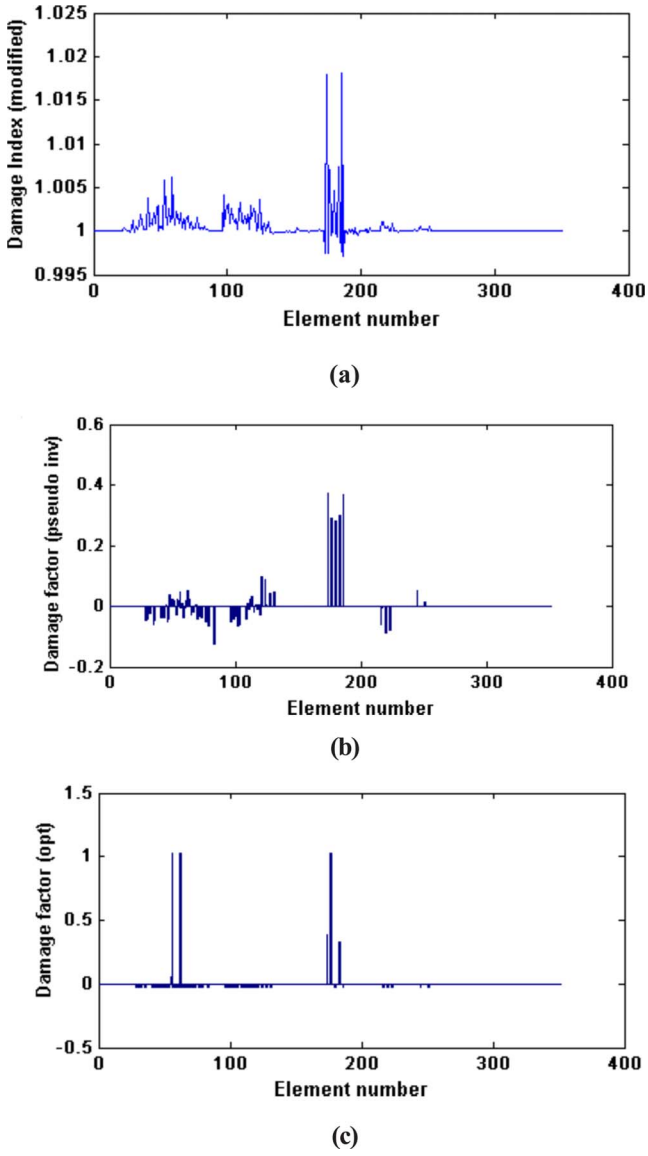

Fig. 9. Results with incomplete modes and measurement errors: (a) damage index (modified); (b) damage factors by matrix update method (pseudo-inverse); and (c) damage factors by matrix update method (optimization)—Damage Case D2

indices using the direct measurements of the modal curvature for 30% damage in Element 3, with different levels of measurement errors in elements of the mode shapes. It is observed that the predictions of the damage location are very accurate even with substantial measurement errors. The effectiveness of curvature-based mode shapes in detecting damage in elements of a girder model is of considerable interest. To the knowledge of the writers, it has not been clearly demonstrated in previous research. The damage indices are calculated for different levels and locations of damage and these indices are used for training a neural network designed for estimating the extent of damage. Details of neural network results are given in the following section.

Application of the Artificial Neural Network Model

The neural network designed for this study is shown in Fig. 2. The method discussed above combines the damage index method and Artificial Neural Network (ANN) to detect the location and severity of damage. In this case the simplified model is used for demonstration. The activation function in the hidden layer is a tangent sigmoid function, while in the output layer it is a pure linear function. The input vector represents the damage indices for the 15 elements, and the single output is the magnitude of damage in the element that is known to have been damaged. For simultaneous damage in two elements the number of neurons in the output layer is increased to two.

The focus of this study is on verifying the performance of the neural network in predicting the damage extent at a given location. It is thus assumed that the damage has already been localized by the damage index method. Three different damage cases are considered: damage only in Element 3, damage only in Element 8, and damage in both Elements 3 and 8. In a practical situation the mode shape measurements would be made only along a few selected degrees of freedom and the measured mode shapes would be contaminated by measurement errors. To ac-

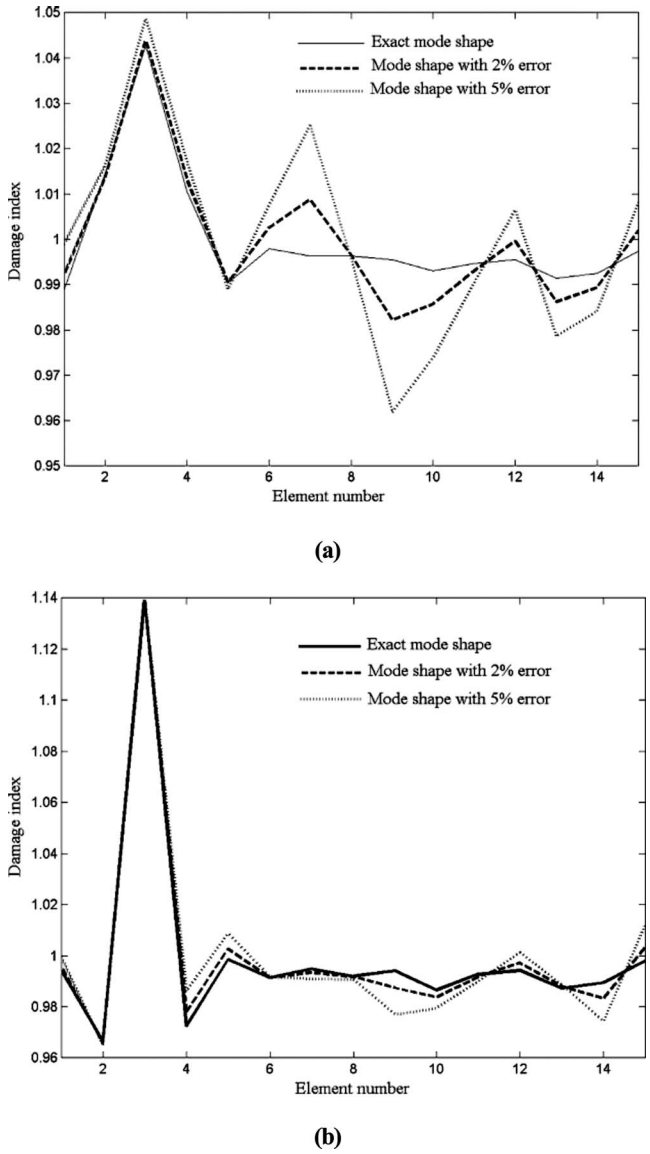

Fig. 10. Damage indices calculated from three modes of Crowchild Bridge girder model with 30% damage in Element No. 3: (a) modal curvatures obtained by numerical differentiations; (b) modal curvatures obtained by direct strain measurements

count for these factors, incomplete mode shapes incorporating only the vertical translation degrees of freedom are used in calculating the damage indices. In addition simulated errors are introduced in the mode shape data by using a random number generator whose states are related to the computer's clock. The errors are assumed to range between −5 and 5%. The designed neural network is trained and then used to assess the damage severity.

Creation of Training Data Set Using Analytical Model

For each damaged element, the damage extent is selected as being 0, 10, 20, 30, 40, 50, or 60%. The corresponding data set of damage indices to be used as input to the neural network is obtained for (1) incomplete mode shapes without error; and (2) incomplete mode shapes with error. In (2), five different error levels are selected for the mode shapes in each damage state. The error levels are −1 to 1%, −2 to 2%, −3 to 3%, −4 to 4%, and −5 to 5%.

Creation of Validation Data Set Using Analytical Model

For each damaged element, the damage extent is selected as being 2, 12, 22, 32, 42, or 52%. As for training, the data set is obtained for incomplete mode shapes with and without error. In the latter case five error levels are selected for the mode shapes at each damage state, namely, −1 to 1%, −2 to 2%, −3 to 3%, −4 to 4%, or −5 to 5%.

Training of the Neural Network

To create a network that can handle the input damage index vectors obtained from incomplete mode shapes with error, it is best to train the network on both accurate and noisy vectors. Thus, the neural network is first trained using a data set obtained from the noisy incomplete mode shapes. This should enable the network to learn how to deal with noise, a common problem in the real world. The network is next trained with a data set obtained from incomplete mode shapes without error. This step is used to maintain the network's ability to deal with accurate input vectors. After the first two steps, which provide initials values for the weights and biases, the network is finally trained with sets that include data obtained from incomplete mode shapes both with and without error. This ensures that the network responds adequately when presented with either ideal or noisy damage index vectors. During each training process, the training is stopped by the validation data set.

Testing of the Trained Neural Network

The reliability of the trained networks is measured by testing the networks with damage index vectors calculated for the various mode shape error levels and six damage severity ranges, that is, 0–10%, 10–20%, 20–30%, 30–40%, 40–50%, and 50–60%. For a single element damage case and for each level of error in the mode shapes between 0 and 8%, 100 different damage index data sets are generated corresponding to each damage severity range. Individual data sets within the same severity and modal error level are different from each other because the magnitudes of errors are changed as the random number generator assigns different errors within the selected error range to the mode shape elements every time the data sets are used. For cases in which two elements are assumed to be damaged 10 pairs of damage extents are selected from the severity ranges defined above. Corresponding to each pair and for each level of mode shape error 10 different damage index sets are generated.

For each damage severity range the network outputs are obtained and relative prediction errors (RPE) are calculated for each mode shape error level. The RPE is defined as the difference between the magnitude of predicted damage and the magnitude of the actual damage. The numbers of outputs within a specific range of RPE are shown in Fig. 11 for a number of selected cases. For example, in Fig. 11(a) for damage <10%, and mode shape error of 1%, about 20 samples out of 100 have a RPE of less than 10%, while about 35 samples have a RPE greater than 50%. Fig. 11(b) for damage extent between 30 and 40% shows that for 1% mode shape error 90 samples out of 100 have RPE less than 10%, while the remaining have RPE between 10 and 20%. Fig. 11(c) for damage extent between 50–60% in two elements show that for up

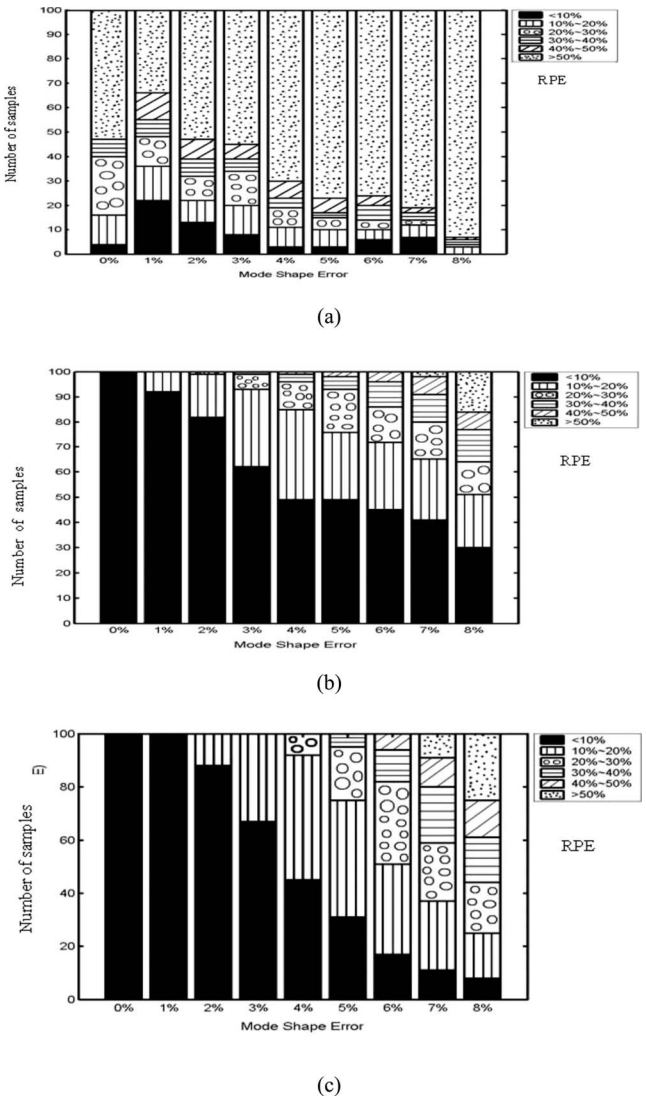

Fig. 11. ANN prediction of error for damage (a) between 0 and 10% in Element 3; (b) damage between 30 and 40% in Element 3; and (c) between 50 and 60% in Elements 3 and 8

to 2% mode shape error, 90% of the samples have RPE less than 10%. It is observed from Fig. 11 that the prediction and generalization capability of the trained neural network is quite good when the damage extent is significant, say, greater than 10%.

Summary and Conclusions

VBDI is a useful tool for SHM. In the past its success has been demonstrated by applications in the damage detection of simple structures. However, its application to real life and complex civil engineering structures is still beset with considerable challenges. The first challenge manifests itself in creating a realistic mathematical model of the structure. This is because structural properties, such as the effective moment of inertia and modulus of elasticity, are quite uncertain and variable, especially in structures built from reinforced concrete where concrete cracking and quality of concrete may have a marked influence on the physical properties. Most modeling attempts, including those used in the present study, use arbitrary estimates of the effective moments of inertia, based on engineering judgment. Correlation of a model which must be based on such choices often requires unrealistic adjustments in the element stiffnesses, even when the differences between the analytical and experimental frequencies are small. In the present case, such adjustments are kept within specified bounds only after the selection of the physical properties was fine tuned by a process of trial and error.

Other challenges include the practical limitation on the degrees of freedom along which modal measurements can be made, the number of modes that can be measured, and the measurement errors that are inevitably present in field tests. As shown here all of these have profound impact on the success of damage identification. In the present study, in order for the methods to succeed, measurements were required along all of the translational degrees of freedom.

Of the many VBDI techniques available only two are used here because of their relative merit in comparison to others. The results obtained form these methods show that in spite of all of the problems, VBDI methods may be successful in identifying at least the location of damage in a civil engineering structure such as the Crowchild Bridge. It is generally not possible to detect damages of small magnitudes through VBDI techniques since the changes in modal properties due to small amounts of damage are not appreciable. Also, if the modal strain energy contribution of an element is very small, even a large degree of damage in it could not be detected by the VBDI techniques. Finally, it should be noted that computer simulation studies cannot quite predict the effect of environmental factors such as temperature changes, changes in boundary conditions, and nonlinearities caused by the opening and closing of cracks and slip in bolted joints. These are potential areas of further research.

The present study has shown that the use of a FE model presents a number of problems in the application of VBDI technique because of the large number of degrees of freedom which do not correspond to the sensor locations, and highly nonuniform distribution of stiffness due to a number of disparate elements in the model. The VBDI technique may be more successful when a simpler and coarser model is used. A simple 15-element girder model of the Crowchild Bridge has been constructed using a continuous beam with equivalent steel sections. In applying the damage index method it is assumed that modal displacements are measured only along the vertical translational degrees of freedom and the modal strain energies are calculated from curvature values obtained by a process of numerical differentiation of the translations. As an alternative, curvatures could be obtained directly by measuring the dynamic strains at two or more points on selected cross sections of the girder model. It is found that location of damage is predicted well even in the presence of significant noise in the measurements, particularly when curvatures are obtained from direct measurements of strains. Once the damage location has been found, a neural network technique provides an estimate of the severity of damage at corresponding locations.

Cheng and Zwol (2005) performed another set of static and dynamic tests on the Crowchild Bridge in 2004. The tests indicated that the overall behavior of the bridge remained unchanged over the last few years and the crack-width in the bridge deck has stabilized. The natural frequencies of the structure have changed slightly (compared to the 1998 test) perhaps due to variations in temperature and boundary conditions (Cheng and Zwol 2005).

This study has demonstrated that a neural network trained with simulated data from FE analysis could be used to determine the damage severity in the girder model of a bridge. The reliability of the damage estimate depends on the amount of the error in the measured mode shapes and the damage severity level. The gen-

eralization capability of the trained network is reliable even for significant errors in the measurement data.

Further study is needed to improve the prediction accuracy for lower damage levels and to find an efficient optimal network architecture, optimum size of the training data set, and effective training algorithm that will enhance the generalization capability of the trained network. The study could also be extended to other types of structural models.

Acknowledgments

The support of the Canadian Network of Centres of Excellence on Intelligent Sensing for Innovative Structures (ISIS Canada) and Fonds québécois de la recherche sur la nature et les technologies is gratefully acknowledged.

Notation

The following symbols are used in this paper:

- a, b = distance of the ends of a beam element from the origin;
- $\mathbf{b}$ = bias vector in a neural network;
- $\mathbf{C}$ = resulting vector of eigenvalue perturbation;
- $\mathbf{D}$ = coefficient matrix relating element stiffness to damage factor;
- d = suffix or superscript to indicate damaged structure;
- E = modulus of elasticity;
- $\mathbf{f}$ = activation functions in a neural network;
- f_{ij} = strain energy factor for element j in mode i of healthy structure;
- f_{ij}^d = strain energy factor for element j in mode i of damaged structure;
- I = moment of inertia;
- i = suffix for mode number;
- J = objective function;
- j = suffix for element number;
- $\mathbf{K}$ = global stiffness matrix;
- $\mathbf{k}_j$ = stiffness matrix for element j;
- L = length of a beam;
- ne = total number of elements in the structural model;
- nm = total number of modes;
- $\mathbf{P}$ = input vector in a neural network;
- $\mathbf{W}$ = weight matrix in a neural network;
- x = linear coordinate;
- β_j = damage factor for element j;
- γ_{ij} = damage index of element j in mode i;
- γ_j = damage index of element j;
- $\bar{\gamma}_j$ = modified damage index of element j;
- λ_i = ith eigenvalue;
- ϕ_i = modal vector corresponding to mode i; and
- ψ'' = modal curvature.

References

Allman, D. J. (1984). "A compatible triangular element including vertex rotations for plane elasticity analysis." *Comput. Struc.*, 19(1–2), 1–8.

Bagchi, A. (2005). "Updating the mathematical model of a structure using the measured vibration characteristics." *J. Vib. Control*, 11(12), 1469–1486.

Bagchi, A., Humar, J., and Noman, A. (2007). "Development of a finite element system for vibration-based damage identification in structures." *J. Appl. Sci.*, 7(17), 2404–2413.

Bakht, B., and Mufti, A. (1998). "Five steel-free bridge deck slabs in Canada." *Struct. Eng. Int. (IABSE, Zurich, Switzerland)*, 8(3), 196–200.

Batoz, J. L. (1982). "An explicit formulation for an efficient triangular plate bending element." *Int. J. Numer. Methods Eng.*, 18, 1077–1089.

Cheng, J. J. R., and Afhami, S. (1999). "Field instrumentation and monitoring of Crowchild Bridge in Calgary, Alberta." *Univ. of Alberta Rep. for ISIS Canada*, Univ. of Alberta, Edmonton, Canada.

Cheng, J. J. R., and Zwol, T. V. (2005). "Steel-free deck: Field performance and evaluation." *Proc., Int. Workshop on Innovative Bridge Deck Technologies*, ISIS Canada Research Network, Winnipeg, Canada.

Doebling, S. W., Farrar, C. R., and Prime, M. B. (1998). "A summary review of vibration-based damage identification methods." *Shock Vib. Dig.*, 30, 91–105.

Farrar, C. R., Baker, W. E., Bell, T. M., Cone, K. M., Darling, T. W., Duffey, T. A., Eklund, A., and Migliori, A. (1994). "Dynamic characterization and damage detection in the I-40 bridge over the Rio Grande." *Rep. No. LA 12767-MS*, Los Alamos National Laboratory, Los Alamos, New Mexico.

Gill, P. E., Murray, W., and Wright, M. H. (1981). *Practical optimization*, Academic, London.

Hagan, M. T., Demuth, H. B., and Beale, M. (1995). *Neural network design*, PWS, Boston.

Humar, J., Bagchi, A., and Xu, H. (2006). "Performance analysis of vibration-based techniques for structural damage identification." *Struct. Health Monit.*, 5(3), 215–241.

Humar, J., Xu, H., and Bagchi, A. (2004). "Application of neural networks in damage detection in structures." *Proc., 2nd Int. Workshop on SHM (SHM 2004)*, ISIS Canada Research Network, Winnipeg, Canada.

Humar, J. L., Bagchi, A., and Xu, H. (2003). "Vibration-based damage identification for a three span continuous steel-free deck bridge located in Canada." *Proc., Int. Workshop on Structural Health Monitoring of Bridges/Colloquium on Bridge Vibration (SHMB)*, Kitami Institute of Technology, Kitami, Japan, 203–210.

Kabe, A. M. (1985). "Stiffness matrix adjustment using mode data." *AIAA J.*, 23(9), 1431–1436.

MATLAB. (2009). *User's guide*, Mathworks Inc., Natick, Mass.

O'Callahan, J., Avitabile, P., and Riemer, R. (1989). "System equivalent reduction expansion process (SEREP)." *Proc., 7th Int. Modal Analysis Conf.*, Society for Experimental Mechanics, Bethel, Conn., 29–37.

Stubbs, N., Kim, J.-T., and Farrar, C. R. (1995). "Field verification of a non-destructive damage localization and severity estimation algorithm." *Proc., 13th Int. Modal Analysis Conf.*, Canadian Society of Civil Engineering, Montreal, 210–218.

Tadros, G., Tromposch, E., and Mufti, A. A. (1998). "Superstructure replacement of the Crowchild Trail Bridge." *Proc., 5th Int. Conf. on Short and Medium Span Bridges*, Society for Experimental Mechanics, Bethel, Conn.

Ventura, C. E., Onur, T., and Tsai, R. C. (2000). "Dynamic characteristics of the Crowchild Trail Bridge." *Can. J. Civ. Eng.*, 27, 1046–1056.

Xu, H., and Humar, J. (2006). "Damage detection in a girder bridge by artificial neural network technique." *Comput. Aided Civ. Infrastruct. Eng.*, 21, 450–464.

Zang, C., and Imregun, M. (2001). "Structural damage detection using artificial neural networks and measured FRF data reduced via principal component projection." *J. Sound Vibrat.*, 242(5), 813–827.